

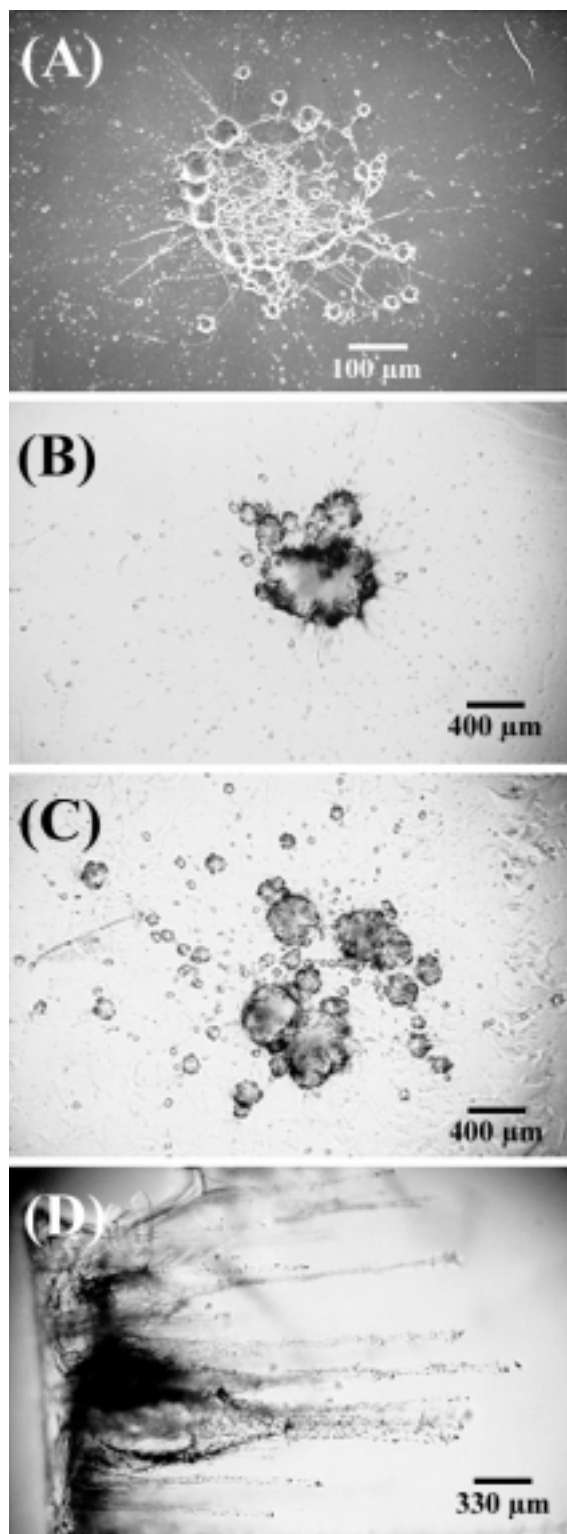
CAPTURE OF POORLY COHESIVE HYPERVELOCITY PARTICLES BY SiO₂ AEROGEL;

F. Hörz ¹, M.J. Cintala ¹, R.P. Bernhard ², and T.H. See ², ¹SN4, NASA – Johnson Space Center, Houston, Texas 77058, horz@snmail.jsc.nasa.gov & mcintala@ems.jsc.nasa.gov, ² Lockheed-Martin Space Mission Systems & Services, C23, 2400 NASA Road 1, Houston, Texas 77058, bernhard@snmail.jsc.nasa.gov & thsee@ems.jsc.nasa.gov.

Introduction: The utility of aerogel as a capture medium for hypervelocity particles has been demonstrated for relatively dense, competent projectiles, such as powdered minerals, or glass and metal-spheres (*e.g.*, 1, 2, 3). Many natural particles may be less competent, and may even include friable objects. Experimental confirmation that such particles can be successfully trapped by aerogel has been elusive, because materials of low compressive or tensile strength tend to disintegrate at gravitational accelerations of 10^6 to 10^7 g that are typically associated with light-gas guns or plasma-drag accelerators. Using a small caliber (5 mm) light-gas gun we developed two methods that simulate the impact of poorly cohesive, if not strengthless, projectiles into aerogel at ~ 6 km/s.

Collisional Disruption: Dispersion angle, grain size, and other properties of debris clouds that emanate down-range from penetrated targets depend systematically on the target thickness (T) relative to the projectile diameter (D_p), as demonstrated from witness-plate observations (4) or from in situ, high-speed optical photography and/or X-radiography (5). Relatively coarse-grained, modestly dispersing beams of projectile fragments emanate from very thin targets ($D_p/T > 10$). Consequently, we collisionally disrupted soda-lime glass spheres ($D_p = 50$ μ m) upon penetration of aluminum foils ($T = 0.8$ to 4 μ m) and intercepted the resulting fragment clouds with aerogel collectors (in lieu of witness plates) located behind the foil. In addition to the impact velocity and foil thickness, we varied the standoff distance (L) of the aerogel specimen relative to the penetrated bumper-foil. At otherwise constant impact conditions, this procedure allowed for the geometric manipulation of the radial separation distance of neighboring fragments, so that either tight clusters or substantially diffuse swarms of fragments would encounter the aerogel collector.

Representative results, using 4 μ m aluminum foils and aerogel collectors of 0.02 g/cm³ density, are illustrated in Figures A-F. A typical, polished Cu-witness plate, at $L = 4$ mm, is shown in Figure A, while Figures B and C represent typical aerogel impacts at $L = 2$ and 15 mm, respectively, all at a constant impact velocity (V) of approximately 6 km/s. Note the increased fragment dispersion with increasing L in Figures B and C. Clearly, the resolution of individual fragment impacts is vastly superior in the metal witness plate compared to aerogel, where closely spaced and overlapping impacts coagulate into massive penetration holes in the brittle aerogel target. Figure D is a cross-section of the event illustrated in Figure C and displays numerous penetration tracks of various lengths, thus attesting to the impact of many particles of variable sizes. Most of the massive tracks in Figure D contain projectile residue in the form of black dots at their tips. Figures E and F show optical and SEM photographs of the aerogel surface for an experiment at $V = 6.6$ km/s and $L = 15$ mm. Note the presence of pro-



AEROGEL CAPTURE OF POORLY COHESIVE PARTICLES: F. Hörz *et al.*

jectile melts in the form of beaded stringers and/or partial loops, and that these strengthless liquids penetrate deeply into the aerogel targets.

Cocoa Powder: When experimenting with 50 μm spheres we typically employ “shot-gunning” methods and load approximately 70-100 projectiles into a small, cylindrical cavity in the sabot. Available evidence suggests that projectile break up during light-gas gun firings occurs inside this cavity. Therefore, we pursued various approaches to reduce the disintegration of the projectiles during launch. One idea included the intimate mixing of projectiles with very fine-grained powders, the latter potentially providing for some beneficial cushioning among neighboring projectiles. These mixtures were gently compressed inside the sabot cavity with a small plunger.

One of the powders utilized was commercial cocoa. Unlike other powders, during free flight, the cocoa broke into numerous, small clods that remained sufficiently coherent to cause distinct, bulbous penetrations upon impact with the aerogel as illustrated in Figure G ($V = 6.2 \text{ km/s}$; aerogel of 0.02 g/cm^3). Long, thin tracks emanating from some of these bulbous cavities are caused by nominal test projectiles (glass) that were part of an impacting cocoa clod, and which penetrate deeper than the low-density, friable cocoa material. All features seen in Figure G are readily reproduced. Figure H illustrates the interior of a single cocoa track — viewed through the entrance hole — and reveals finely distributed cocoa powder. Detailed chemical analyses of these residues are being conducted elsewhere.

Caveat: The impact velocity for such projectiles cannot be determined precisely. However, it should be close to measured projectile velocity for the collisionally produced fragment clouds based on (5). The impact of cocoa clods with the aerogel produces measurable light flashes, detected via photodiodes and recorded by high-speed oscilloscopes. The oscilloscope traces reveal a substantial distribution of impact velocities, with the earliest events being consistent with the expected projectile velocity, while the last arrivals are some 30-50% slower.

Conclusions: Friable, porous particles, composed of compacted powders and totally strengthless, tightly clustered particle beams and melts yield morphologically distinct penetration features in aerogel targets. They also leave analyzable residues at impact velocities of $\sim 6 \text{ km/s}$, the typical encounter velocity expected for the Discovery Class STARDUST sample return mission to comet Wild 2.

References: (1) Tsou, P. (1995) *J. Non-Crystalline Solids*, 186, 415-427; (2) Nishioka, K. *et al.* (1994), *LPI Technical Report 94-05*, 61-64; (3) Barrett, R. *et al.* (1992), *Proc. Lunar Planet. Science Conf.*, 22nd, 203-212; (4) Hörz, F. *et al.* (1994) *Int. J. Impact Engng.*, 15, 257-280; (5) Piekutowski, A. (1993) *Int. J. Impact Engng.*, 14, 573-586.

